

Accepted Manuscript

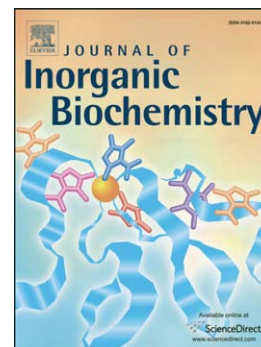
Siderophore inspired tetra- and octadentate antenna ligands for luminescent Eu(III) and Tb(III) complexes

Lena J. Daumann, Philipp Werther, Michael J. Ziegler, Kenneth N. Raymond

PII: S0162-0134(16)30008-3
DOI: doi: [10.1016/j.jinorgbio.2016.01.006](https://doi.org/10.1016/j.jinorgbio.2016.01.006)
Reference: JIB 9895

To appear in: *Journal of Inorganic Biochemistry*

Received date: 1 October 2015
Revised date: 5 January 2016
Accepted date: 7 January 2016



Please cite this article as: Lena J. Daumann, Philipp Werther, Michael J. Ziegler, Kenneth N. Raymond, Siderophore inspired tetra- and octadentate antenna ligands for luminescent Eu(III) and Tb(III) complexes, *Journal of Inorganic Biochemistry* (2016), doi: [10.1016/j.jinorgbio.2016.01.006](https://doi.org/10.1016/j.jinorgbio.2016.01.006)

This is a PDF file of an unedited manuscript that has been accepted for publication. As a service to our customers we are providing this early version of the manuscript. The manuscript will undergo copyediting, typesetting, and review of the resulting proof before it is published in its final form. Please note that during the production process errors may be discovered which could affect the content, and all legal disclaimers that apply to the journal pertain.

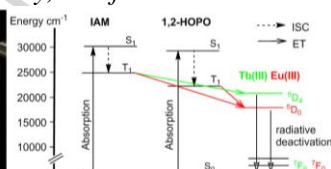
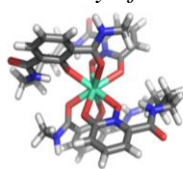
Graphical Abstract

Three antenna ligands bearing 1,2-hydroxypyridonate (HOPO) and 2-hydroxisophthalamide (IAM) chromophores are reported. Photophysical characterization of the Gd(III), Eu(III) and Tb(III) complexes revealed localized triplet states for the chromophores and that they need to reside on a primary amine of the spermine backbone to be efficient in lanthanide excitation.

Siderophore inspired tetra- and octadentate antenna ligands for luminescent Eu(III) and Tb(III) complexes

Lena J. Daumann, Philipp Werther, Michael J. Ziegler and Kenneth N. Raymond

Chemical Sciences Division, Lawrence Berkeley National Laboratory, Berkeley, California 94720, and Department of Chemistry, University of California, Berkeley, California 94720



Leave this area blank for abstract info.



ELSEVIER

Siderophore inspired tetra- and octadentate antenna ligands for luminescent Eu(III) and Tb(III) complexes

Lena J. Daumann, Philipp Werther, Michael J. Ziegler and Kenneth N. Raymond

Chemical Sciences Division, Lawrence Berkeley National Laboratory, Berkeley, California 94720, and Department of Chemistry, University of California, Berkeley, California 94720

In memory of Professor Graeme Hanson and his contributions to Bioinorganic Chemistry and Electron Paramagnetic Resonance

ARTICLE INFO

Article history:

Received

Received in revised form

Accepted

Available online

Keywords:

luminescent lanthanides

siderophore inspired ligands

antenna

Europium

Terbium

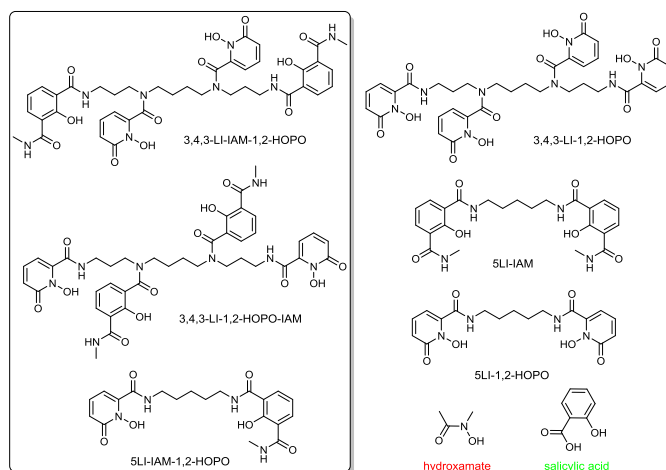
ABSTRACT

Following the success of the siderophore-inspired 1,2-hydroxypyridonate (HOPO) and 2-hydroxisophthalamide (IAM) chromophores in Eu(III) and Tb(III) luminescence, we designed three new ligands bearing both chromophores. Syntheses of the octadentate ligands 3,4,3-LI-IAM-1,2-HOPO and 3,4,3-LI-1,2-HOPO-IAM, where the chromophores are attached to different positions in the (LI = linear) spermine backbone, are reported in addition to a tetradentate ligand based on 1,5-diaminopentane. The Gd(III) complexes were prepared and revealed localized triplet states typical for the IAM and HOPO chromophores. Photophysical characterization of the Eu(III) and Tb(III) complexes revealed that the chromophores need to reside at a primary amine of the spermine backbone to be efficient in lanthanide excitation. These systems help us to understand the antenna effect in siderophore inspired chromophores and could be potential targets for sensing and biological imaging applications.

1. Introduction

Lanthanides (Ln) (or rare earth elements (REE) when including Sc and Y)[1] are featured in a multitude of applications in technology,[2-6] research[7] and medicine[8-10] and have recently been found to have a role in nature as metalloenzymes.[11-13] It is especially due to their favorable luminescent properties (long lifetimes, narrow emission bands, large effective Stokes' shifts) that they have found their way in many applications, like dissociation enhanced lanthanide fluorescence immunoassay (DELFLIA), homogeneous time resolved fluoroimmunoassays (HTRF) and luminescence resonance energy transfer (LRET) assays.[14, 15] In consequence of their forbidden f-f-transitions, indirect excitation via an organic chromophore (antenna effect) is employed. Siderophore inspired ligands have been used to efficiently chelate Ln and actinides (Ac). For example, the octadentate ligand 3,4,3-LI-1,2-HOPO (Figure 1, LI stands for a linear, unbranched ligand backbone) based on the spermine backbone, has been reported to be an excellent actinide sequestering agent *in vivo*. [16-20] However, due to the high acidity of the 1,2-hydroxypyridonate (1,2-HOPO) moieties in this ligand, mixed 1,2-HOPO and catechol amide (CAM) or 3,2-HOPO spermine ligands have been developed.[21-23] By altering the chelating moieties, different affinities and stabilities in various pH can be achieved. 3,4,3-LI-1,2-HOPO has also been reported as being an excellent antenna for sensitizing both Ln and Ac.[16, 20, 24] The hydroxamate inspired 1,2-HOPO chromophore has been shown to be an especially efficient sensitizer for Eu(III) luminescence, with

photoluminescence quantum yield (Φ_{tot}) as high as 20% for the tetradentate 5LI-1,2-HOPO ligand, while the salicylate-type IAM chromophore triplet state is better matched to sensitize Tb(III) with excellent quantum yields of 36% with the tetradentate 5LI-IAM ligand or as high as 60% in octadentate IAM cages in



aqueous solution.[14, 25]

Figure 1 New siderophore inspired ligands (left) and previously reported highly efficient antenna and f-element sequestering ligands (right)

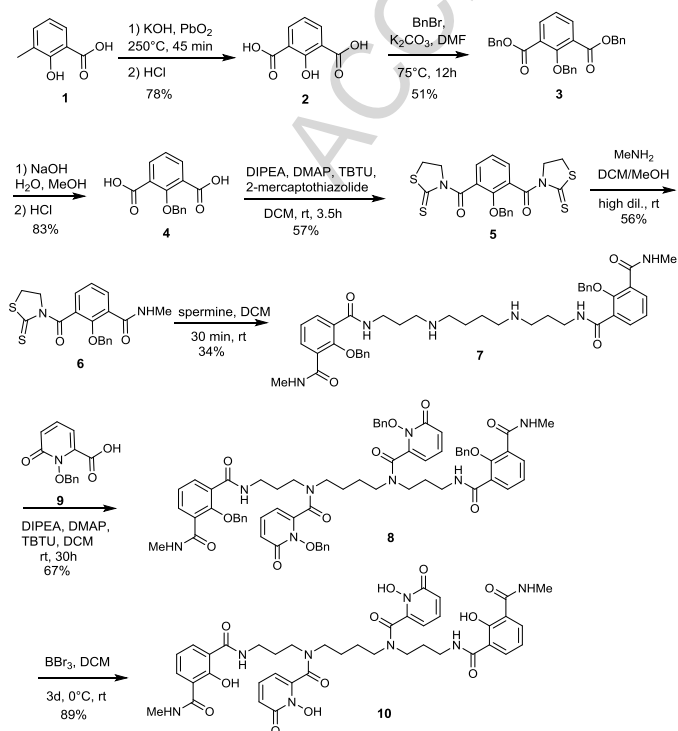
Here we report the synthesis of three new ligands (Scheme 1-3), two octadentate and one tetradentate, based on the IAM and 1,2-HOPO chelating chromophores (Figure 1) and discuss the effects of different antennas on photophysical properties such as Φ_{tot} and triplet state to aid design and deeper understanding of new luminescent probes and sequestering agents. The Eu(III) and Tb(III) complexes of the reported ligands have been characterized by high resolution Electrospray Injection Mass Spectrometry (ESI-MS) and photophysical measurements. In addition, a new and more efficient synthesis to the previously reported benzyl protected IAM precursor is reported here. Density Functional Theory (DFT) calculations were conducted to elucidate the structure around the metal ions and to assess the ligand abilities to fully coordinate the metal ions.

2. Experimental

2.1 Materials and Methods

Ground state density functional theory (DFT) calculations were performed at the Molecular Graphics and Computational Facility, College of Chemistry, University of California, Berkeley using Gaussian 09.[26] The ground state geometries of the complexes were optimized using the B3LYP functional, treating the light atoms with the 6-31G(d,p) basis set and the Eu(III) with the effective core potential MWB52.[27, 28] *Nuclear Magnetic Resonance (NMR)* spectra were obtained using (unless otherwise noted) a Bruker AV600 spectrometer operating at 600 (151) MHz for ^1H (or ^{13}C , respectively). ^1H (or ^{13}C) chemical shifts are reported in ppm relative to the solvent resonances, taken as δ 7.26 (77.0), 2.50 (39.5) and 4.78 (49.2), respectively for CDCl_3 , $(\text{CD}_3)_2\text{SO}$ and CD_3OD while coupling constants (J) are given in Hz. *Fourier-Transform Infra-Red (FT-IR)* spectroscopy was conducted using a Nicolet 380 spectrometer from Thermo Electron (ZnSe crystal). High-Resolution Electrospray Ionization (HR-ESI)-Mass spectrometry was performed at the QB3/Chemistry Mass Spectrometry Facility, University of California, Berkeley.

2.2 Ligand and Complex Syntheses



Scheme 1 Synthesis of 3,4,3-LI-IAM-1,2-HOPO (10).

CAUTION The coupling reagent *O*-(Benzotriazol-1-yl)-*N,N,N',N'*-tetramethyluronium tetrafluoroborate (TBTU) used in some of the syntheses is potentially explosive and should be handled with care.

2-Hydroxyisophthalic acid (2). This compound was synthesized after a slight modification of a previously published procedure.[29] Potassium hydroxide (115 g, 2.05 mol) was combined with water (24 mL) in a stainless steel beaker and 3-methylsalicylic acid **1** (19.2 g, 0.126 mol) and lead(IV) oxide (115 g, 0.481 mol) were added. The mixture was stirred with a glass rod and heated to 250°C for 45 min. Subsequently the orange mixture was cooled to ~ 100°C and poured into water (1 L). Orange lead(II) oxide and red lead were filtered off on a glass frit. The filtrate was partially neutralized (pH~10) with concentrated hydrochloric acid (150 mL) and saturated sodium sulfide was added until no further precipitation of black lead(II) sulfide occurred. The black solution was heated briefly to coagulate lead(II) sulfide (40°C, 10 min) and the black suspension filtered through a glass frit. Subsequently the filtrate was acidified to pH 1 with concentrated hydrochloric acid (120 mL) while cooling on ice to precipitate 2-hydroxyisophthalic acid (**2**) as white solid. The product was collected on a glass frit and first dried in air and then in high vacuum overnight. Yield 17.91 g (78 %). ^1H NMR (DMSO, 400 MHz): δ 6.89 (t, 1H, J = 7.7 Hz), 7.94 (d, 2H, J = 7.7 Hz). ^{13}C NMR (d^6 -DMSO, 150 MHz) δ 117.5; 118.1; 135.9; 162.0; 169.4. FTIR (ν , cm^{-1}) 2968 (b, O-H str); 1687 (s, C=O str); 1154 (s, C-O str); 755 (m, arH). n-ESI HRMS (MeOH): 181.0142 (calc. 181.0142, $[\text{C}_8\text{H}_5\text{O}_5]^-$, [M-H]).

Dibenzyl-2-(benzyloxy)isophthalate (3). This compound was synthesized after a modification of a previously published procedure.[30] 2-Hydroxyisophthalic acid (**2**) (5.0 g, 0.027 mol), dry potassium carbonate (15.18 g, 0.109 mol) and benzyl bromide (18.78 g, 0.109 mol, 13.06 mL) were added to dimethylformamide (DMF, 35 mL) in a flame dried flask under a nitrogen atmosphere. The reaction mixture was stirred for 16 h at 75°C. Subsequently the solution was cooled down to room temperature, filtered and the solid washed with DMF (5 x 1 mL). The filtrate was evaporated to dryness in high vacuum (60°C water bath) to yield a yellow, viscous oil. The crude product was purified by column chromatography (SiO_2 , gradient from 0 % to 10 % MeOH in dichloromethane). Purified **3** crystallized after drying in high vacuum as yellow needles. Yield 6.32 g (51 %). ^1H NMR (CDCl_3 , 400 MHz) δ 5.04 (s, 2H), 5.29 (s, 4H), 7.21 (t, 1H, J = 7.7 Hz), 7.29-7.35 (m, 15H), 7.96 (d, 2H, J = 7.7 Hz). ^{13}C NMR (CDCl_3 , 150 MHz) δ 67.2; 77.9; 123.7; 127.3; 127.8; 128.2; 128.3; 128.4; 128.5; 135.0; 135.6; 136.8; 158.0; 165.5. IR (ν , cm^{-1}) 3033, 2946 (m, CH_2 str); 1720 (s, C=O str); 1248 (s, C-O-C str); 734 (m, arH). p-ESI HRMS (MeOH) 453.1695 (calc. 453.1697, $[\text{C}_{29}\text{H}_{25}\text{O}_5]^+$); 475.1514 (calc. 475.1516, $[\text{C}_{29}\text{H}_{25}\text{NaO}_5]^+$).

2-(benzyloxy)isophthalic acid (4). This compound was synthesized after a modification of a previously published procedure.[30] Dibenzyl 2-(benzyloxy)isophthalate (**3**) (2.91 g, 6.43 mmol) was dissolved in methanol (50 mL) and sodium hydroxide (0.771 g, 19.3 mmol, in 8 mL water) were added. In order to dissolve the starting material completely, more methanol (13 mL) was added and the solution was sonicated (final solvent composition: MeOH/ H_2O 8/1). Subsequently the mixture was stirred at room temperature for 17 h. The solvent was removed *in vacuo*, then the residue was co-evaporated first with water (15 ml) then diethyl ether (15 mL). The yellow residue was taken up with half saturated sodium chloride solution (50 mL) and extracted with dichloromethane (2 x 25 mL). Starting material

was recovered from the combined and dried organic phases. The aqueous phase was acidified to pH 1 with concentrated hydrochloric acid and the white precipitate of (**4**) was filtered and dried *in vacuo* overnight. Yield: 1.46 g (83 %). ¹H NMR (DMSO, 600 MHz) δ 5.03 (s, 2H); 7.29-7.39 (m, 4H); 7.47 (d, 2H, J = 7.0 Hz); 7.84 (d, 2H, J = 7.7 Hz), 13.25 (bs, 2H). ¹³C NMR (DMSO, 150 MHz) δ 76.7; 123.9; 128.1; 128.4; 128.6; 133.7; 137.4; 156.4; 167.5; 176.0. IR (ν, cm⁻¹) 2870 (b, O-H str); 2685 (m, CH₂ str); 1720 (s, C=O str); 1244 (s, C-O-C str); 766 (m, arH). n-ESI HRMS (MeOH): 271.0609 (calc. 271.0612, C₁₅H₁₁O₅⁻, [M-H]⁻).

2-(Benzyloxy)-1,3-phenylenebis((2-thioxothiazolidin-3-yl)methanone (5)). 2-(Benzyloxy)isophthalic acid (**4**) (2.00 g, 7.35 mmol), 2-mercaptothiazoline (1.84 g, 15.4 mmol), 4-dimethylaminopyridine (DMAP, 80.8 mg, 661 μmol), TBTU (5.66 g, 17.6 mmol) were dissolved in dichloromethane (60 mL). After addition of *N,N*-diisopropylethylamine (DIPEA, 3.80 g, 29.4 mmol, 5.13 mL), the mixture turned yellow immediately, and was stirred at room temperature for 3.5 h. After removal of the solvent *in vacuo*, **5** was purified with column chromatography (SiO₂, 100 % dichloromethane (DCM)) to afford a yellow powder. Yield 2.00 g (57 %). ¹H NMR (CDCl₃, 400 MHz) δ 3.02 (t, 4H, J = 7.3 Hz), 4.41 (t, 4H, J = 7.3 Hz), 5.02 (s, 2H), 7.21 (t, 1H, J = 7.7 Hz), 7.31-7.40 (m, 5H), 7.48 (d, 2H, J = 7.6 Hz). ¹³C NMR (CDCl₃, 100 MHz) δ 29.2, 56.1, 77.6, 124.2, 128.1, 128.9, 129.2, 132.6, 136.7, 153.8, 167.6, 201.2. IR (ν, cm⁻¹) 2939 (m, CH₂ str); 1673 (s, C=O str); 1221 (s, C-O str); 1148 (s, C-S str); 752 (m, arH). p-ESI HRMS (MeOH) 497.0081 (calc. 497.0092, [C₂₁H₁₈N₂NaO₃S₄]⁺).

2-(Benzyloxy)-*N*-methyl-3-(2-thioxothiazolidine-3-carbonyl)benzamide (6). A solution of methylamine (1.7 mL, 3.39 mmol, 2M in tetrahydrofuran (THF)) in DCM/MeOH (95:5, 200 mL) was added slowly over 48 h to a solution of **5** (1.61 g, 3.39 mmol) in 5 mL dichloromethane using a syringe pump. After removal of the solvent, the yellow residue was dissolved in dichloromethane (50 mL) and was washed with 1M KOH solution (2 x 30 mL). The combined organic phases were dried and the solvent was removed under reduced pressure. Subsequently the crude (**6**) was purified by column chromatography (SiO₂, gradient from 0 % to 10 % EtOAc in DCM) to yield 0.74 g (56 %) of **6** as a yellow powder. ¹H NMR (CDCl₃, 400 MHz) δ 2.85 (d, 3H, J = 4.9 Hz), 3.14 (t, 2H, J = 7.3 Hz), 4.51 (t, 2H, J = 7.3 Hz), 4.98 (s, 2H), 7.27 (t, 1H, J = 7.7 Hz), 7.34-7.41 (m, 5H), 7.48 (dd, 1H, J = 7.6, 1.8 Hz), 8.14 (dd, 1H, J = 7.8, 1.8 Hz). ¹³C NMR (CDCl₃, 100 MHz) δ 26.8; 28.9; 55.9; 78.5; 125.1; 127.9; 128.3; 129.1; 129.1; 129.9; 132.6; 134.6; 136.1; 154.5; 165.6; 167.7; 201.8. p-ESI HRMS (MeOH) 387.0825 (calc. 387.0832, [C₁₉H₁₉N₂O₃S₂]⁺); 409.0644 (calc. 409.0651, [C₁₉H₁₈N₂NaO₃S₂]⁺); 425.0385 (calc. 425.0390, [C₁₉H₁₈KN₂O₃S₂]⁺).

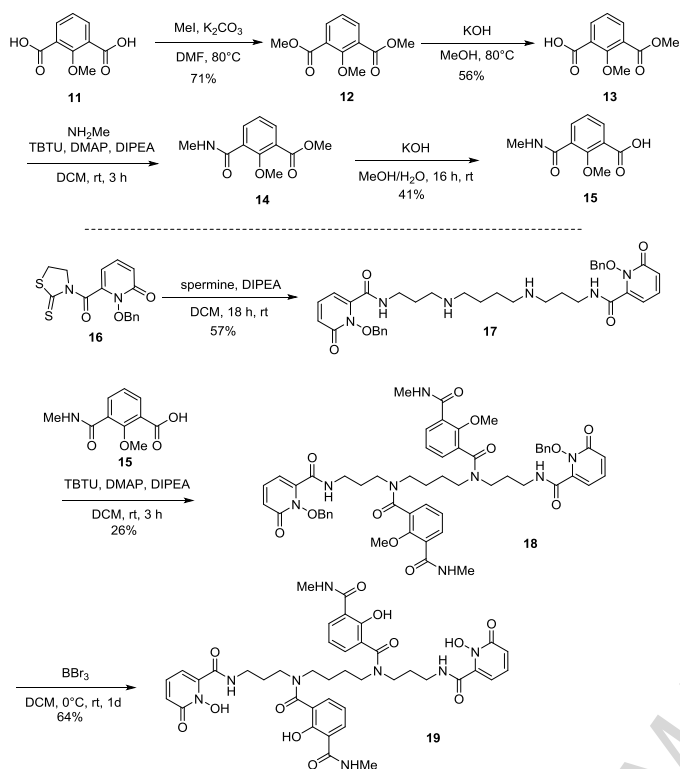
3,4,3-LI-IAMBn (7). A solution of **6** (988 mg, 2.56 mmol) and DIPEA (0.424 mL, 2.43 mmol) in dichloromethane (300 mL) was added dropwise at room temperature over 24h to a solution of spermine (254 mg, 1.22 mmol) in dichloromethane (35 mL). After the complete addition, the reaction mixture was stirred for another 24h. Subsequently the solvent was removed from the colorless solution under reduced pressure and the crude product was subjected to column chromatography (Al₂O₃ basic, gradient 0% to 10% MeOH in dichloromethane) to yield 3,4,3-LI-IAMBn (**7**) as a white solid. Yield: 308 mg (34%). ¹H NMR (CDCl₃, 600 MHz) δ 1.36 (m, 4H), 1.62 (p, 4H, J = 6.4 Hz), 2.44 (m, 4H), 2.57 (t, 4H, J = 6.4 Hz), 2.88 (d, 6H, J = 4.8 Hz), 3.45 (q, 4H, J = 6.1 Hz), 4.94 (s, 4H), 7.26 (t, 2H, J = 7.7 Hz), 7.34-7.41 (m, 10H), 7.49-7.52 (m, 2H), 7.94-7.95 (m, 4H), 7.98-8.00 (m, 2H). ¹³C NMR (CDCl₃, 150 MHz) δ 26.9, 28.0, 29.2, 39.1, 48.1, 49.8,

79.4, 125.4, 129.0, 129.0, 129.1, 129.2, 129.5, 133.9, 134.0, 135.6, 154.5, 165.9, 166.3 p-ESI HRMS (MeOH) 737.4023 (calc. 737.4021, [C₄₂H₅₃N₆O₆]⁺); 369.2050 (calc. 369.2047, [C₄₂H₅₄N₆O₆]²⁺).

3,4,3-LI-IAMBn-1,2-HOPOBn (8). 3,4,3-LI-IAMBn (**7**) (362 mg, 491 μmol), 1,2-HOPOBn (**9**) [16] (289 mg, 1.18 mmol), DMAP (5.4 mg, 44 μmol), TBTU (379 mg, 1.18 mmol) were suspended in 20 ml DCM. DIPEA (254 mg, 1.96 mmol, 343 μL, ρ 0.74 g/cm³) was added to start the reaction and it was stirred at room temperature for 30 h until TLC showed no further conversion. After removal of the solvent under reduced pressure, the crude product was subjected to column chromatography (SiO₂, gradient from 0 % to 10 % MeOH in DCM) to afford a white solid. Yield: 394 mg (67 %). ESI MS, LC-ESI MS data as well as TLC experiments indicated partial cleavage of benzyl protecting groups during the purification step. Thus the crude (**8**) was used directly in the next step. p-ESI HRMS (MeOH): 1191.5160 (calc. 1191.5186, [C₆₈H₇₁N₈NaO₁₂]⁺); 1213.4967 (calc. 1213.5005, [C₆₈H₇₀N₈NaO₁₂]⁺); 1229.4748 (calc. 1229.4745, [C₆₈H₇₀N₈KO₁₂]⁺).

3,4,3-LI-IAM-1,2-HOPO (10). 3,4,3-LI-IAMBn-1,2-HOPOBn (**8**) (206 mg, 173 μmol) was dissolved in dry dichloromethane (5 mL) and cooled on an ice bath. Boron tribromide (1.73 g, 6.92 mmol, 656 μL, ρ 2.64 g/cm³) was added and the mixture was stirred overnight and allowed to warm to room temperature. Subsequently the solvent and excess boron tribromide were removed under high vacuum. The orange residue was cooled with liquid nitrogen and methanol was added until no further gas evolution was observed (ca. 50 mL). The solution was allowed to warm to room temperature and refluxed for 2.5 h. Then the solution was concentrated (to ca 1 mL) and filtered. Diethyl ether was added to the filtrate to precipitate a beige solid. The solvent was removed *in vacuo* and orange oily residue of **10** was dried in high vacuum. Yield 128 mg (89 %). ¹H NMR (CD₃OD, 600 MHz) δ 1.49-2.01 (m, 8H), 2.93 (bs, 6H), 2.95 (s, 3H), 3.46-3.64 (m, 8H), 3.30-3.31 (m, 4H), 6.53-6.85 (m, 4H), 6.96 (s, 2H), 7.46-7.71 (m, 2H), 7.91-8.00 (m, 4H). n-ESI HRMS (MeOH) 829.3135 (calc. 829.3162, [C₄₀H₄₅N₈O₁₂]⁻). IR (ν, cm⁻¹) 2868 (m, CH₂ str); 1631, 1527 (s, C=O str); 1431 (m, CH₂ def); 795, 756 (m, arH).

2-Methoxy-3-(methoxycarbonyl)benzoic acid (13) 2-Methoxyisophthalic acid (**11**) (2.75 g, 14.0 mmol) and K₂CO₃ (5.81 g, 42.1 mmol) were suspended in DMF (50 mL). Methyl iodide (2.6 mL, 5.97 g, 42.1 mmol) was added slowly at room temperature. After the mixture was stirred at 80°C overnight, the solvent was evaporated *in vacuo*. The solid residue was dissolved in DCM (150 mL) and washed with water and brine (50 mL, respectively). The organic layer was dried over Na₂SO₄ and the solvent was removed to deliver dimethyl 2-methoxyisophthalate (**12**) as a yellow oil (2.24 g, 71 %), which was used directly in the next step. The yellow oil (1.28 g, 5.7 mmol) was dissolved in methanol (15 mL) and KOH (320mg, 5.7 mmol) was added. The mixture was refluxed for 4 h, and then concentrated *in vacuo*. The solid residue was dissolved in water (5 mL) and the aqueous layer was acidified with 6M HCl solution until an off-white oil separated. The aqueous layer was extracted with DCM (3x20 mL). The organic layers were combined, washed with water and brine and dried over Na₂SO₄. The solvent was evaporated and 2-methoxy-3-(methoxycarbonyl)benzoic acid **13** was obtained as a white solid. Yield: 673 mg (56 %) ¹H-NMR (CDCl₃, 400 MHz) δ 3.96 (s, 3H), 4.05 (s, 3H), 7.33 (t, 1H, J = 8.5 Hz), 8.08 (d, 1H, J = 8.5 Hz), 8.30 (d, 1H, J = 8.5 Hz), 11.1 (bs, 1H).



Scheme 2 Synthesis of 3,4,3-LI-1,2-HOPO-IAM (19).

Methyl 2-methoxy-3-(methylcarbamoyl)benzoate (14) 2-methoxy-3-(methoxycarbonyl)benzoic acid (**13**) (516 mg, 2.45 mmol) was dissolved in DCM (5 mL). TBUTU (1.97 g, 6.14 mmol), DMAP (0.75 mg, 6.14 mmol) and methylamine (2M in THF, 3.68 mL, 7.36 mmol) were added. The reaction was started by adding DIPEA (214 μ L, 159 mg, 1.23 mmol) and stirred for 3 h at room temperature. The solvent was evaporated and column chromatography (SiO₂, DCM:MeOH, 0-10 % gradient) delivered methyl 2-methoxy-3-(methylcarbamoyl)benzoate as an off-white liquid. Yield: 770 mg (140 %, contained TBUTU impurity). ¹H NMR (CDCl₃, 600 MHz) δ 3.03 (d, 3H, J = 5.0 Hz), 3.89 (s, 3H), 3.94 (s, 3H), 7.25-7.28 (m, 1H), 7.67-7.72 (bs, 1H), 7.91 (d, 1H, J = 8.2 Hz), 8.24 (d, 1H, J = 8.2 Hz). p-ESI HRMS (MeOH) 224.0914 (calc. 224.0917, [C₁₁H₁₄O₄N]⁺)

2-Methoxy-3-(methylcarbamoyl)benzoic acid (15) Methyl 2-methoxy-3-(methylcarbamoyl) benzoate (**14**) (770 mg, 3.45 mmol) was dissolved in methanol (5 mL). An aqueous 1 M KOH solution (5.17 mL, 5.17 mmol) was added and the mixture was stirred at room temperature for 16 h. The solvent was evaporated and the solid residue redissolved in water (5 mL). The aqueous layer was extracted with DCM (3 x 5 mL), and then acidified with 6 M HCl solution. A yellowish oil separated, which was extracted with DCM (3 x 15 mL). The organic layers were combined, dried over Na₂SO₄ and the solvent was evaporated to yield 2-methoxy-3-(methylcarbamoyl)benzoic acid (**15**) as a white solid. Yield: 296 mg (41 %) ¹H NMR (CDCl₃, 600 MHz) δ 3.05 (d, J = 5.0 Hz, 3H), 3.94 (s, 3H), 7.31 (t, 1H, J = 7.2 Hz), 7.60-7.65 (bs, 1H), 8.10 (d, J = 7.2 Hz, 1H), 8.25 (d, J = 7.2 Hz, 1H). ¹³C NMR (CDCl₃, 150 MHz) δ 27.1, 64.0, 123.8, 124.8, 128.2, 135.5, 136.6, 136.7, 158.4, 165.6. p-ESI HRMS (MeOH) 210.0757 (calc. 210.0761 for C₁₀H₁₂N⁺).

3,4,3-Li-1,2-HOPOBn (17) 1,2-HOPOBn thiazolide (**16**) (1.78 g, 5.4 mmol) and DIPEA (0.87 mL, 0.66 g, 5.1 mmol) were dissolved in DCM (100 mL) and added over 1 h to a solution of

spermine (519 mg, 2.6 mmol) in DCM (50 mL). The mixture was stirred for 18h at rt until TLC showed full conversion. The reaction mixture was washed with 1M KOH (2 x 150 mL) solution, subsequently concentrated *in vacuo*. The crude product was purified with column chromatography (Al₂O₃ basic, 0.5% MeOH in dichloromethane) yielding the pure product (**17**) as yellowish residue. Yield: 968 mg (57 %). ¹H NMR (CDCl₃, 600 MHz) δ 1.27 (m, 4H), 1.66 (m, 4H), 2.15 (s, 2H), 2.31 (m, 4H), 2.55 (m, 4H), 3.41 (s, 4H), 5.92 (s, 4H), 6.35 (d, J = 6.2 Hz, 2H), 6.64 (d, J = 10.2 Hz, 2H), 7.26 (dd, J = 6.2, 7.2 Hz, 2H), 7.22-7.55 (m, 10H) 8.55 (bs, 2H) ¹³C NMR (CDCl₃, 150 MHz) δ 27.0, 27.1, 39.2, 47.7, 48.2, 79.4, 105.9, 123.6, 138.2, 128.5, 129.5, 130.4, 138.3, 143.3, 158.6, 160.3. p-ESI HRMS m/z 657.3387 (calc. 657.3395 for C₃₆H₄₅O₆N₆⁺).

3,4,3-Li-1,2-HOPOBn-IAMMe (18) 3,4,3-Li-1,2-HOPOBn (**17**) (220 mg, 335 μ mol) was dissolved in DCM (60 mL). TBUTU (231 mg, 720 μ mol), DMAP (4 mg, 33 μ mol) and 2-methoxy-3-(methylcarbamoyl)benzoic acid (**15**) (141 mg, 720 μ mol) were added. The reaction was started by adding DIPEA (234 μ L, 173 mg, 1.34 mmol) and stirred for 3 h at room temperature. The solvent was evaporated and column chromatography (SiO₂, DCM:MeOH 0-10%) yielded the protected ligand 3,4,3-Li-1,2-HOPOBn-IAMMe as a white solid. Yield 92 mg (26 %). ESI MS, LC-ESI MS data as well as thin layer chromatography (TLC) experiments indicated partial cleavage of benzyl protecting groups during the purification step. Thus the crude (**18**) was used directly in the next step. p-ESI HRMS m/z 1039.4555 (calc. 1039.4560 for C₅₆H₆₃O₁₂N₈⁺).

3,4,3-Li-1,2-HOPO-IAM (19) The protected 3,4,3-Li-1,2-HOPOBn-IAMMe ligand (403 mg, 388 μ mol) was dissolved in dry DCM (10 mL) under inert conditions and cooled on ice. Neat BBr₃ (1.47 mL, 3.89 g, 15.5 mmol) was slowly added and the mixture was warmed up to room temperature and stirred overnight. The solvent was evaporated *in vacuo*. The solid residue was quenched with methanol while cooling with liquid nitrogen. After no further reaction could be observed, the reaction was heated to reflux for 3 h in an open flask, while adding constantly methanol to maintain a steady level. The mixture was concentrated to ~1 mL and filtrated. Addition of diethylether precipitated the deprotected ligand 3,4,3-Li-1,2-HOPO-IAM (**19**) as a brown residue, which was dried *in vacuo*. Yield: 303 mg (64 %). ¹H NMR (CD₃OD, 600 MHz) δ 1.22-1.91 (m, 8H); 2.79 (d, 6H); 2.93-3.56 (m, 12H); 6.37-7.62 (m, 12H). n-ESI HRMS m/z 829.3237 (calc. 829.3162 for C₄₀H₄₅O₁₂N₈⁻ (L-H)). IR (v, cm⁻¹) 2830 (m, CH₂ str); 1631, 1526 (s, C=O str); 1432 (m, CH₂ def); 794, 747 (m, arH).

Syntheses of the Eu^{III} and Tb^{III} complexes The complexes were synthesized following a general procedure: A ~1M solution of LnCl₃·6H₂O (0.9 eq, 29.2 μ mol) in methanol was prepared and added to a solution of **10** or **19** (1 eq, 32.5 μ mol) in methanol (~3 mL) by what a white precipitate was formed instantaneously. After stirring for 5 min, pyridine (10 eq, 325 μ mol) was added and the mixture was heated at 60°C for two hours. Subsequently, the mixture was cooled down to room temperature and centrifuged. The residue was extracted with methanol (2 x 3 mL) in order to remove uncoordinated ligand and the white solid was dried in high vacuum.

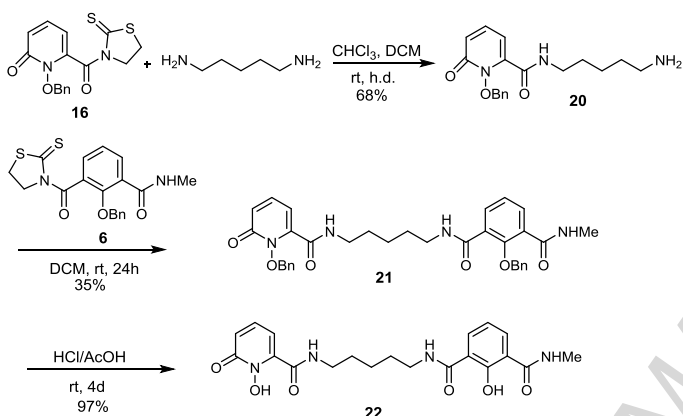
[Eu(3,4,3-LI-IAM-1,2-HOPO)]C₅H₅NH Yield: 39 %. n-ESI HRMS (MeOH) 979.2124 (calc. 979.2140, [EuC₄₀H₄₂N₈O₁₂]). IR (v, cm⁻¹) 1598, 1540 (s, C=O str); 1433 (m, CH₂ def); 1180 (m, C-OH, str); 801, 762, 696 (m, arH, pyH).

[Tb(3,4,3-LI-IAM-1,2-HOPO)]C₅H₅NH Yield: quantitative. n-ESI HRMS (MeOH) 985.2167 (calc. 985.2181,

[TbC₄₀H₄₂N₈O₁₂]. IR (ν, cm⁻¹) 2969 (m, CH₂ str); 1588, 1530 (s, C=O str); 1433 (m, CH₂ def); 1170 (m, C-OH, str); 801, 762, 696 (m, arH, pyH).

[Eu(3,4,3-LI-1,2-HOPO-IAM)]PyH Yield: 78 %. n-ESI HRMS (MeOH) 977.2106 (calc. 977.2126, [EuC₄₀H₄₂O₁₂N₈]). IR (ν, cm⁻¹) 2969 (m, CH₂ str); 1588, 1530 (s, C=O str); 1433 (m, CH₂ def); 1170 (m, C-OH, str); 801, 762, 696 (m, arH, pyH).

[Tb(3,4,3-LI-1,2-HOPO-IAM)]PyH Yield: 28 %. n-ESI HRMS (MeOH) 985.2183 (calc. 985.2181, [TbC₄₀H₄₂O₁₂N₈]). IR (ν, cm⁻¹) 2959 (m, CH₂ str); 1598, 1520 (s, C=O str); 1433 (m, CH₂ def); 1151 (m, C-OH, str); 801, 753, 645 (m, arH, pyH).



Scheme 3 Synthesis of 5LI-IAM-1,2-HOPO (**22**).

5LI-1,2-HOPOBn (20). 1,2-HOPOBn thiazolide (**16**) (1 g, 2.9 mmol) was dissolved in chloroform (150 mL) and added over 20 hours to a solution of 1,5-diaminopentane (1.3 g, 12.7 mmol) in dichloromethane (5 mL) at room temperature using a syringe pump. The solution was stirred overnight and subsequently washed with 1M NaOH in 20% brine (3x 100 mL), brine (2x 100 mL) and then dried over sodium sulfate. The solvent was removed in high vacuum and the pale brown oil was dried in high vacuum for two days. Yield 650 mg, 68%. ¹H NMR (CDCl₃) δ 1.26 (m, 2H); 1.36 (m, 2H); 1.45 (m, 2H); 2.57 (m, 2H); 3.29 (m, 2H); 5.25 (s, 2H); 6.39 (d, 1H); 6.63 (dd, 1H); 7.19-7.45 (m, 8H); 7.69 (s, 1H). ¹³C-NMR (150 MHz, CDCl₃) δ (ppm) 24.0, 28.7, 30.2, 40.0, 41.4, 79.3, 106.6, 123.8, 127.9, 128.6, 129.4, 130.1, 138.8, 142.8, 158.1, 160.1. p-ESI HRMS (MeOH) 330.1811 (calc. 330.1812, [C₁₈H₂₄N₃O₃]⁻).

5LI-IAMBn-1,2-HOPOBn (21). 5LI-1,2-HOPOBn (**20**) (125 mg, 0.38 mmol) and IAMMeNBn thiazolide (**6**) (123 mg, 0.32 mmol) were dissolved in dichloromethane (5 mL) and stirred at room temperature for 24 hours. The pale yellow solution was then evaporated and the crude oil purified with column chromatography (100% DCM, then 5% MeOH in DCM). **21** was obtained as a beige oil. Yield 67 mg, 35%. ¹H NMR (CDCl₃) δ 1.29 (m, 2H); 1.31 (m, 2H); 1.50 (m, 2H); 2.91 (d, 3H); 3.29 (m, 4H); 4.82 (s, 2H); 5.22 (s, 2H); 6.30 (dd, 1H); 6.54 (d, 1H); 7.13-7.39 (m, 14H); 7.48 (d, 1H); 7.83 (dd, 2H). ¹³C-NMR (150 MHz, CDCl₃) δ (ppm) 23.2, 26.6, 27.6, 28.6, 39.7, 78.5, 79.4, 105.9, 123.7, 124.9, 128.4, 128.5, 128.7, 128.9, 129.2, 129.4, 130.2, 133.1, 133.3, 133.4, 135.2, 138.1, 142.9, 153.9, 158.5, 160.3, 165.6, 166.5. p-ESI HRMS (MeOH) 619.2511 (calc. 619.2527, [C₃₄H₃₆N₄O₆Na]⁺).

5LI-IAM-1,2-HOPO (22). 5LI-IAMBn-1,2-HOPOBn (**21**) (67 mg, 0.11 mmol) was dissolved in a 1:1 mixture of concentrated hydrochloric acid and glacial acetic acid (2 mL) and stirred at room temperature for four days. The solvent was removed in high vacuum and then the beige oil co-evaporated with MeOH to yield **22** as a beige foam. Yield 47 mg, 97% ¹H

NMR (MeOD, 600 MHz) δ 1.40 (m, 2H); 1.59 (m, 2H); 2.28 (s, 3H); 3.28-3.40 (m, 4H); 6.48 (d, 1H); 6.64 (d, 1H); 6.88 (t, 1H); 7.38 (dt, 1H); 7.88 (m, 2H). p-ESI HRMS (MeOH) 415.1619 (calc. 415.1623, [C₂₀H₂₃N₄O₆]). IR (ν, cm⁻¹) 1637, 1529 (s, C=O str); 1429 (m, CH₂ def); 1154 (m, C-O-H str); 804, 754 (m, arH).

Eu(III) and Tb(III) complexes of 5LI-IAM-1,2-HOPO (**22**)

Due to the low quantity of ligand obtained, the complexes were made *in situ* for photophysical measurements. Two equiv. of ligand were dissolved in DMSO (0.01 M) and one equivalent of LnCl₃ solution in DMSO (0.05 M) was added. Subsequently, ten equivalents of pyridine were added and the solutions left to equilibrate at room temperature prior to mass spectrometric analysis and photophysical measurements.

[Eu(5LI-IAM-1,2-HOPO)₂]⁻ p-ESI HRMS (MeOH) 979.2262 (calc. 979.2283, [C₄₀H₄₄EuN₈O₁₂]⁻).

[Tb(5LI-IAM-1,2-HOPO)₂]⁻ p-ESI HRMS (MeOH) 987.2319 (calc. 987.2338, [C₄₀H₄₄TbN₈O₁₂]⁻).

2.3 Photophysical Measurements

Sample preparation for absorption, Φ_{tot}, ε and τ measurements: The complexes of the octadentate complexes were dissolved in DMSO (1 mg/ml) or *in situ* generated in the same solvent in case of the tetradentate complexes and then diluted into tris(2-aminoethyl)amine (TRIS) buffered saline (TBS) (20 mM buffer, pH 7.4, 100 mM NaCl) to a final concentration of ~0.5 × 10⁻⁵ M. **UV-visible absorption** spectra were recorded with an HP 8453 diode array UV-vis absorption spectrometer. Relative quantum yields were determined by the optically dilute method (eq (1)) using the same excitation wavelength for both the reference (Quinine Sulfate, purchased from Sigma-Aldrich, meets USP testing specifications) and samples (λ_{ex} = 330 nm) following a previously described protocol in aqueous medium.[16, 31] Please note, that we used a previously described protocol from our group here for determination of Φ_{tot} for consistency. However, it should be mentioned that optimized protocols are now available.[32-34] Quinine sulfate (QS) in 0.5 M H₂SO₄ (Φ = 0.546) was used as the aqueous fluorescence quantum yield standard.[31]

$$\frac{\Phi_x}{\Phi_{QS}} = \left[\frac{A_{QS}(\lambda_{QS})}{A_x(\lambda_x)} \right] \left[\frac{E_x}{E_{QS}} \right] \quad \text{eq (1)}$$

A is the absorbance at the excitation wavelength (λ) and E is the integrated photoluminescence intensity. The subscripts 'x' and 'QS' refer to the sample and reference respectively. The plot of integrated emission intensity (*i.e.* E_{QS}) vs. absorbance at 330 nm (*i.e.* A_{QS}) yields a linear plot with a slope which can be equated to the quinine sulfate quantum yield Φ_{QS}. [31] Instrumentation details (HORIBA Jobin Yvon IBH FluoroLog-3 spectrofluorimeter) and protocols were the same as recently published. Time-gated phosphorescence spectra of the *in situ* generated gadolinium complexes were measured in methanol:ethanol (1:4 v/v) at 77 K (λ_{ex} = 330 nm, delay: 0.1 ms) using the same HORIBA Jobin Yvon IBH FluoroLog-3 spectrofluorimeter. The Gd-triplet phosphorescence spectra were fitted using Gaussian functions with OriginPro 6.1 software.[35, 36] The *in situ* preparation protocol was as follows: One equivalent of **10** or **19** or two equivalents of **22** were dissolved in MeOH (0.01 M), respectively, and one equivalent of GdCl₃ hexahydrate solution in MeOH (0.05 M) was added. Subsequently, ten equivalents of pyridine were added and the solutions left to equilibrate at room temperature prior to mass spectrometric analysis and photophysical measurements. To confirm successful formation of the Gd(III) complexes *in situ*, n-

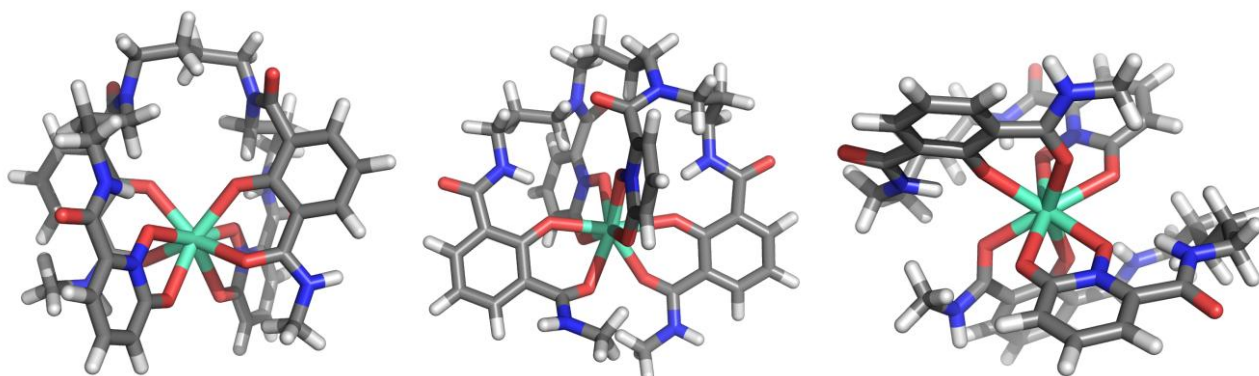


Figure 2 DFT optimized structures of the Europium complexes of the three mixed ligands.

ESI HRMS were recorded of the samples in methanol. Spectra are included in the supporting information.

$[\text{Gd}(\text{5LI-IAM-1,2-HOPO})_2]^-$ n-ESI HRMS (MeOH) 986.2330 (calc. 986.2325, $[\text{C}_{40}\text{H}_{44}\text{GdN}_8\text{O}_{12}]^-$).

$[\text{Gd}(3,4,3\text{-LI-IAM-1,2-HOPO})]^-$ n-ESI HRMS (MeOH) 984.2172 (calc. 984.2169, $[\text{GdC}_{40}\text{H}_{42}\text{N}_8\text{O}_{12}]^-$).

$[\text{Gd}(3,4,3\text{-LI-1,2-HOPO-IAM})]^-$ n-ESI HRMS (MeOH) 984.2172 (calc. 984.2169, $[\text{GdC}_{40}\text{H}_{42}\text{N}_8\text{O}_{12}]^-$).

3. Results and Discussion

3.1. Ligand and Complex Syntheses

The octadentate ligand syntheses, characterization and purification proved to be challenging (Schemes 1 and 2), due to 1) rotamer formation (visible in the $^1\text{H-NMR}$ spectra) of the 3,4-3-LI-IAMBn and 3,4,3-LI-1,2-HOPOBn precursors, 2) the decreased nucleophilicity of the secondary amines in 3,4-3-LI-IAMBn and 3,4,3-LI-1,2-HOPOBn due to formation of intramolecular hydrogen bonds and thus decreased reactivity in the final coupling step. This has been previously observed in spermine based, mixed 1,2-HOPO/catechol ligands, leading to yields as low as 5%. [22] Thus a different activating mechanism was considered and the coupling reagent TBTU yielded the best results with up to 70% yield. 3) We observed partial cleavage of the benzylic protecting groups which occurred during purification of **7** and **17** and thus full NMR characterization was conducted after deprotection with BBr_3 (which was found to be superior to HCl/AcOH deprotection for the octadentate ligands). The tetradentate 5LI-IAM-1,2-HOPO ligand was obtained under high dilution/slow addition conditions in moderate yield (Scheme 3). The ligands and complexes were, among other methods, characterized by HR-ESI-mass spectrometry and the corresponding spectra can be found in the supporting information. The complexes were observed in the negative ion

mode and for the complexes with octadentate ligands adducts with HBr were found in the addition to the $[\text{ML}]^-$ species. The free octadentate ligands also showed formation of HBr adducts. The high affinity for anions has been previously observed for IAM ligands and complexes like the $\text{BH}(2,2)\text{IAM}$ cage. [25]

3.2. DFT calculations

Despite considerable efforts, no X-ray suitable crystals were obtained for the complexes. We thus conducted geometry optimizations to assess the ability of the ligands to fully coordinate $\text{Ln}(\text{III})$ ions. Input structures were based on recently published crystal structures of $\text{Eu}(\text{III})$ complexes of related 3,4,3-LI-1,2-HOPO and 5LIO-1,2-HOPO ligands. [16, 37] The structures are shown in Figure 2 and demonstrate the ability of the ligands to shield the metal ions efficiently from solvent molecules.

3.3. Photophysical characterization

Matching the triplet state of an antenna to the emitting state of a lanthanide is one of the key factors in designing highly luminescent reporter molecules. [14, 38] Although in theory the singlet state can also transfer energy to the lanthanide ion, the short lifetime makes this pathway less efficient and is thus considered of little importance. [39, 40] In the IAM chromophore for example the lowest singlet and triplet states are close in energy ($\Delta S_1\text{-T}_{0,0} = 850\text{ cm}^{-1}$) favoring a high rate of intersystem crossing and an excitation via the triplet state. [14] For 1,2-HOPO excitation via the triplet state is also considered to be the dominating pathway. [41] In order to determine the triplet states of the ligands, phosphorescence spectra were collected of the gadolinium complexes of the mixed IAM-1,2-HOPO ligands at 77K (Figure 3). This ion lacks ligand accessible states for energy transfer and thus only ligand centered phosphorescence is observed from which one can deduce the ligand's triplet state.

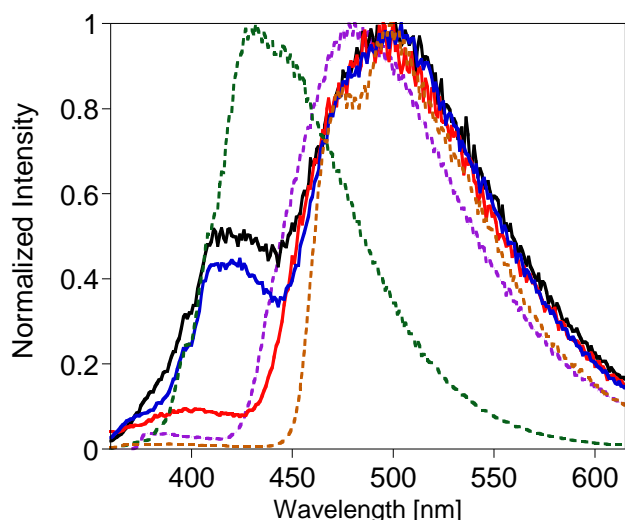


Figure 3 Phosphorescence spectra at 77K in MeOH/EtOH (1:4). [Gd(3,4,3-LI-1,2-HOPO)] (purple, dashed line), [Gd(3,4,3-LI-IAM-1,2-HOPO)] (black, solid line), [Gd(3,4,3-LI-1,2-HOPO-IAM)] (red, solid line), [Gd(5LI-IAM-1,2-HOPO)] (blue, solid line), [Gd(5LI-IAM)] (green, dashed line), [Gd(5LI-1,2-HOPO)] (orange, dashed line).

For completeness, the spectra of the 5LI-IAM, 5LI-1,2-HOPO and 3,4,3-LI-1,2-HOPO complexes were also recorded under the same conditions and are included in Figure 3. The herein experimentally determined triplet state for the 5LI-IAM ligand (24400 cm^{-1}) is in good agreement with the values previously reported and demonstrates why this chromophore is such an excellent sensitizer for terbium (${}^5\text{D}_4 = 20500\text{ cm}^{-1}$, $\Delta T_1-{}^5\text{D}_4 = 2750-3900\text{ cm}^{-1}$). In order to facilitate efficient energy transfer (ET), the gap between the lanthanide emitting state and the antenna's triplet state should be greater than 2000 cm^{-1} otherwise significant energy back transfer (EBT) can occur.

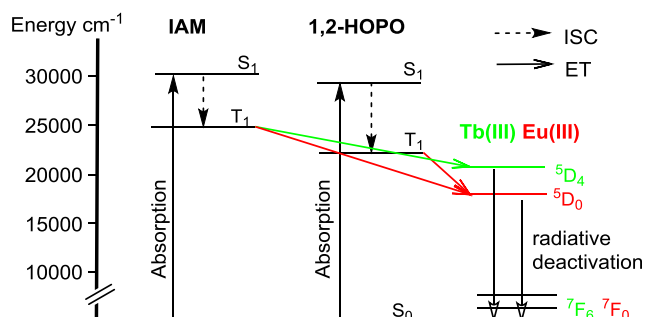


Figure 4 Energy level diagram showing energy transfer pathways from the different chromophores to the emissive states of Eu(III) and Tb(III). The red arrows (\rightarrow) indicate that ET can occur both from the IAM and 1,2-HOPO triplet states for Eu(III) while for Tb(III) excitation from IAM is proposed to be the main pathway (\rightarrow). In addition, Tb(III) can transfer energy back onto the 1,2-HOPO triplet state after excitation by IAM. Energy back transfer pathways not shown for clarity.

The triplet state of the previously reported octadentate 3,4,3-LI-1,2-HOPO ligand is slightly higher (22400 cm^{-1}) than the one of 5LI-1,2-HOPO (21500 cm^{-1}) but both ligands are well suitable to act as antenna for europium (${}^5\text{D}_0 = 19030\text{ cm}^{-1}$, $\Delta T_1-{}^5\text{D}_0 = 3370-2470\text{ cm}^{-1}$). While the IAM chromophore has been reported as moderately efficient antenna for europium[42] ($\Delta T_1-{}^5\text{D}_0 \sim 4800\text{ cm}^{-1}$), the 1,2-HOPO chromophore is not suited as terbium sensitizer, due to the small energy gap ($\Delta T_1-{}^5\text{D}_4 \sim 1000\text{ cm}^{-1}$). In

this work, we observed for the tetradentate mixed chromophore ligand 5LI-IAM-1,2-HOPO **22** two distinctly separated peaks at 24300 and 21500 cm^{-1} in the phosphorescence spectrum, that correspond well to the triplet states in single chromophore (IAM or 1,2-HOPO) ligands. In the mixed 3,4,3-LI-IAM-1,2-HOPO **10** ligand a similar scenario is observed with both the IAM and 1,2-HOPO triplet states (25300 and 21500 cm^{-1}) being observed. In the 3,4,3-LI-1,2-HOPO-IAM ligand **19**, however, the IAM chromophore phosphorescence is of low intensity (at 25200 cm^{-1}). It is suggested this is due to the importance for this chromophore to reside on a primary amine (yielding a secondary amide bond with the spermine backbone) rather than on a secondary amine of the backbone. Furthermore, due to the closely spaced triplet states of 1,2-HOPO and IAM triplet-triplet ET might also be possible (Figure 4). Interestingly, the absorbance spectrum of [Eu(3,4,3-LI-IAM-1,2-HOPO)] (dashed black line, Figure 5) is blue shifted compared to the complexes with ligands **19** and **22**, indicating a different singlet state energy for ligand **10**. We have also recorded the excitation spectra (Figure S10) and while the complexes follow the same trend (**10** blue shifted in respect to complexes with **19** and **22**), the maxima of the excitation spectra of the complexes are all slightly red-shifted in comparison to the absorbance spectra, which is in accordance with previous data for the 3,4,3-LI-1,2-HOPO complex. The

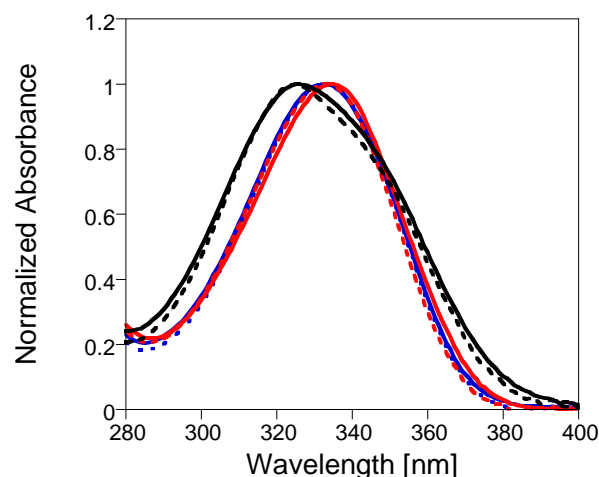


Figure 5 Absorbance spectra of Eu(III) (solid lines) and Tb(III) (dashed lines) of the complexes with 5LI-IAM-1,2-HOPO (**22**) (blue), 3,4,3-LI-1,2-HOPO-IAM (**19**) (red) and 3,4,3-LI-IAM-1,2-HOPO (**10**) (black) in TBS, pH 7.4

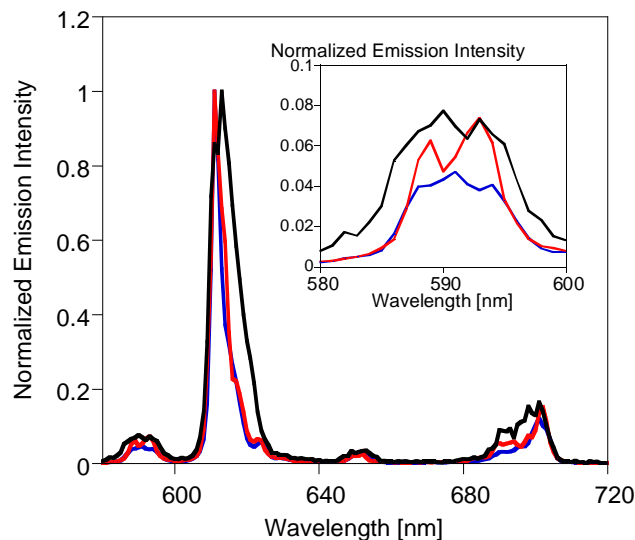


Figure 6 Europium emission spectra of the complexes in TBS, pH 7.4, $\lambda_{\text{ex}} = 330\text{ nm}$. Inset: close-up view of the MD-transition, with the ligands 5LI-IAM-1,2-HOPO (**22**) (blue), 3,4,3-LI-1,2-HOPO-IAM (**19**) (red) and 3,4,3-LI-IAM-1,2-HOPO (**10**) (black).

Table 1 Photophysical data of the complexes

complex	k_{rad} [s ⁻¹]	τ_{rad} [μs]	η_{Eu}	η_{sens}	Φ_{tot} [%]	q	τ_{H_2O} [ms]	τ_{D_2O} [ms]	k_{nonrad} [s ⁻¹]	T_{0-0} [cm ⁻¹]	ϵ [M ⁻¹ cm ⁻¹]	λ_{max} [nm]	bright- ness [M ⁻¹ cm ⁻¹]
[Eu(5LI-IAM-1,2-HOPO) ₂] ⁺	502	1992	0.357	0.119	4.3	0.2	0.71	1.08	904	24300, 21500	24004	335	103
[Tb(5LI-IAM-1,2-HOPO) ₂] ⁺	-	-	-	-	0.5	-	-	-	-	-	21024	334	11
[Eu(3,4,3-LI-1,2-HOPO-IAM)] ⁺	472	2119	0.308	0.016	0.5	0.0	0.65	0.79	1061	25200, 21321	18814	334	9
[Tb(3,4,3-LI-1,2-HOPO-IAM)] ⁺	-	-	-	-	0	-	-	-	-	-	16987	333	-
[Eu(3,4,3-LI-IAM-1,2-HOPO)] ⁺	478	2093	0.242	0.009	0.2	0.3	0.51	0.71	1495	25300, 21500	16171	326	3
[Tb(3,4,3-LI-IAM-1,2-HOPO)] ⁺	-	-	-	-	2.3	-	-	-	-	-	16998	325	39
[Eu(3,4,3-LI-1,2-HOPO)] ⁺ [16]	586	1705	0.469	0.397	15.6	0.04	0.81	1.14	623	22400	17700	315	276
[Eu(5LI-1,2-HOPO) ₂] ⁺ [41]	620	1476	0.490	0.420	20.7	0.05	0.74	0.99	740	21500	18800	331	389
[Tb(5LI-IAM) ₂] ⁺ [42]	-	-	-	-	36.0	-0.1	2.52	2.81	-	24400	25100	337	903

emission spectra recorded are shown in Figure 6 for Eu(III) and in the supporting information for Tb(III) (Figure S11). The former complexes show pure red luminescence due to the band ~612 nm. Interestingly the complex with 3,4,3-LI-IAM-1,2-HOPO (**10**) shows a shift and significant broadening of the hypersensitive ⁵D₀-⁷F₂ transition, indicating a different geometry around the Eu ion with this ligand.[43] Photoluminescence quantum yield (Φ_{tot}) measurements of the europium and terbium complexes of the mixed ligands revealed that the ligands were poor antennas when 1,2-HOPO and IAM chromophores were combined. The tetradentate 5LI-IAM-1,2-HOPO ligand was better in sensitizing europium with a Φ_{tot} of 4.3% than terbium (0.5%) but inferior to 5LI-1,2-HOPO (Eu Φ_{tot} = 21%) and 5LI-IAM (Tb Φ_{tot} = 36%).[44, 45] The 3,4,3-LI-1,2-HOPO-IAM ligand was better than the 3,4,3-LI-IAM-1,2-HOPO ligand in sensitizing europium (Eu Φ_{tot} = 0.5 and 0.2%, respectively). A *vice versa* trend was observed for terbium (Tb Φ_{tot} = 0 and 2.3%, respectively). This is attributed to the fact that the chromophore bound to the secondary amines in the spermine backbone plays a less important role as sensitizer which was shown previously in the 3,4,3-LI-1,2-HOPO ligand, where the R₂N-1,2-HOPO chromophore is less efficient in sensitizing Eu than the RNH-1,2-HOPO chromophore.[16] We propose that the poor ability of the ligands to sensitize terbium is due to two main pathways. Firstly, the energy of the IAM chromophore could be partially transferred to the 1,2-HOPO chromophore which lies too close to the emitting state of terbium. Secondly, when IAM transfers the energy onto terbium, EBT to the 1,2-HOPO causes non-radiative quenching, which is proposed to be the main pathway. Moreover, the triplet state population of the IAM chromophore is negligible (Figure 3, red spectrum) and explains further why the 3,4,3-LI-1,2-HOPO-IAM ligand is not suitable as terbium antenna. To rule out that the low Φ_{tot} of the mixed ligand complexes are due to non-radiative quenching from water molecules, we conducted lifetime measurements in TBS and D₂O. Quenching of lanthanide luminescence by vibrational modes of coordinating solvent molecules is an important factor when designing luminescent probes. Since O-D oscillators are less likely to contribute to non-radiative quenching, the number of water molecules (q) can be deduced from the lifetimes in water (τ_{H_2O}) and deuterated water (τ_{D_2O}), respectively, and using the empirically derived equation (2) from Horrocks *et al.*[46, 47]

$$q_{Eu} = 1.11(\Delta k_{obs} - 0.31) \quad \text{eq (2)}$$

$$\Delta k_{obs} = \frac{1}{\tau_{H_2O}} - \frac{1}{\tau_{D_2O}} \text{ in ms}^{-1} \quad \text{eq (3)}$$

The lifetime measurements for the europium complexes revealed that no water molecules are bound to the complexes in aqueous solution,[46] and that all three ligands are effective in shielding the complexes from quenching water molecules. This is in line with the DFT geometry optimizations described above. It should be noted, however, that the decay of the octadentate Eu(III) complexes could be better fit to a bi-exponential decay, and suggested the presence of a small portion of a short lived species. The presence of multiple species is not unusual has been previously reported for octadentate 1,2-HOPO ligands.[48] Further analysis of the europium emission data was conducted after previously reported methods by Beeby *et al* and Werts *et al*, [49, 50] where Φ_{tot} is the product of the europium centered efficiency (η_{Eu}) and the efficiency of the ligand (η_{sens})

$$\Phi_{tot} = \eta_{Eu}\eta_{sens} \quad \text{eq (4)}$$

$$\eta_{Eu} = \frac{\tau_{H_2O}}{\tau_{rad}} \quad \text{eq (5)}$$

The europium centred efficiency, or sometimes also called intrinsic quantum yield, is significantly (25-50%) lower in the mixed complexes than in complexes with 5LI-1,2-HOPO. Simultaneously, the ligand centred sensitization efficiency (η_{sens}) is lower and follows a certain trend: 5LI-IAM-1,2-HOPO (**22**) > 3,4,3-LI-1,2-HOPO-IAM (**19**) > 3,4,3-LI-IAM-1,2-HOPO (**10**). The almost two-fold higher η_{sens} in **19** compared to **10** confirms the previous observation that the R₂N-1,2-HOPO chromophore is less efficient in sensitizing Eu than the RNH-1,2-HOPO chromophore.[16] The radiative lifetime (τ_{rad}) is the approximated lifetime in the absence of non-radiative processes and can be obtained from the estimated radiative lifetime constant k_{rad}

$$k_{rad} = \frac{1}{\tau_{rad}} = A_{MD,0}n^3 \left(\frac{I_{tot}}{I_{MD}} \right) \text{ in s}^{-1} \quad \text{eq (6)}$$

$A_{MD,0}$ is the spontaneous emission probability of the magnetic dipole transition (⁵D₀-⁷F₁) and is equal to 14.65 s⁻¹, n refers to the refractive index of the medium (here, water = 1.334) and the last term is the ratio of integrated emission intensity of the total emission (⁵D₀-⁷F_J, J = 0-6) divided by the integrated ⁵D₀-⁷F₁ emission (580-600 nm).[50-53] Please note, due to experimental limitations the ⁵D₀-⁷F₅ and ⁵D₀-⁷F₆ transitions were not recorded and we stress that the total emission intensity I_{tot} is thus only a low estimate. Shortening τ_{rad} has been discussed as being one of the most important steps in generating highly emissive europium complexes.[43, 54] The data shown in Table 1

confirms this claim. Finally, the rate of non-radiative decay (k_{nonrad}) can be deduced from the lifetime in water ($\tau_{\text{H}_2\text{O}}$) and k_{rad} .

$$k_{\text{nonrad}} = k_{\text{obs}} - k_{\text{rad}} = \frac{1}{\tau_{\text{obs}}} - \frac{1}{\tau_{\text{rad}}} \text{ in s}^{-1} \text{ eq (7)}$$

Compared to the 3,4,3-LI-1,2-HOPO ligand, non-radiative decay rates of the two mixed octadentate ligands are twofold enhanced.[16] Keeping in mind that quenching through water molecules is not the main pathway; the data in Table 1 suggests that the antenna itself contributes to the quenching of the luminescence. ET between the closely spaced triplet states (and possibly also the singlet states) of IAM and 1,2-HOPO and EBT between europium and the two chromophores leads to the poor photophysical performance of the complexes. This result is surprising as previously groups have reported the use of synergistic two-antenna systems, where either a protein serves as first antenna which then transferred the energy onto an organic chromophore or where two chromophores (e.g. hfac and *N,N*-dimethyl-*N,N*-bis(2-hydroxy-3,5-dimethylbenzyl)ethylenediamine) were combined.[20, 55-57] We stress, that the above analysis of our systems is by far not exhaustive and that other quenching mechanisms and factors such as pre-equilibration of the triplet state might be alternative mechanisms that can explain the photophysical properties of our systems.[58] Another interesting aspect of the systems reported here is the pH dependence of the luminescence intensity for the octadentate 3,4,3-LI-IAM-1,2-HOPO complexes (Figure S12). The luminescence intensity increases upon raising the pH from 6.5-8.5 and could be potentially exploited for pH sensing applications. One reason for this increase in luminescence upon raising the pH could be the deprotonation of potentially quenching N-H or O-H oscillators. Finally, the brightness of the complexes was determined from the product of the molar extinction coefficient ϵ and Φ_{tot} and was for all mixed chromophore complexes lower than previously reported 1,2-HOPO or IAM complexes.[25, 37, 48]

4. Conclusion

We report the first synthesis of three ligands incorporating both the IAM and 1,2-HOPO chromophores. While none of the three ligands achieve the high quantum yields as the homochromophoric systems, the three hetero-chromophoric ligands provided us with a greater understanding of the photophysical properties of siderophore inspired antenna ligands. Specifically, when bound to a terminal primary amine of the spermine backbone, the chromophores (IAM or 1,2-HOPO) were better in sensitizing the respective ions (Tb or Eu). Moreover, we have observed that including multiple different antennas does not necessarily lead to a synergistic antenna effect in these systems. The interesting pH-dependence and ability to bind anions (e.g. HBr), however, could make the system useful for applications as sensors. In addition, the octadentate ligands could prove to be useful as actinide sequestration agents.

Acknowledgments

This work was supported by the Director, Office of Science, Office of Basic Energy Sciences, and the Division of Chemical Sciences, Geosciences, and Biosciences of the U.S. Department of Energy at LBNL under Contract No. DE-AC02-05CH11231. LJD is grateful for a fellowship of the Alexander von Humboldt foundation. PW and MJZ wish to acknowledge PROMOS scholarships of the German Academic Exchange Service (DAAD). The Molecular Graphics and Computation Facility is supported by the NSF CHE-0233882 and CHE-0840505 grants. The authors thank Dr. Nicola Alzakhem for helpful discussions.

Note Some of this technology is licensed to Lumiphore, Inc. in which KNR has a financial interest.

Supplementary Material

ESI-Mass spectra of the Eu(III), Tb(III) and Gd(III) complexes, additional emission spectra and excitation spectra are available in the supporting information.

References

- [1] D.A. Atwood, *The rare earth elements: fundamentals and applications*, John Wiley & Sons, (2013).
- [2] V. Fernandez-Moreira, B. Song, V. Sivagnanam, A.-S. Chauvin, C.D.B. Vandevyver, M. Gijs, I. Hemmila, H.-A. Lehr, J.-C.G. Bünzli, *Analyst*, 135, (2010), 42-52.
- [3] J.-C.G. Bünzli, S.V. Eliseeva, *Chem. Sci.*, 4, (2013), 1939-1949.
- [4] J.C.G. Bünzli, *Chem. Rev. (Washington, DC, U. S.)*, 110, (2010), 2729-2755.
- [5] S.J. Butler, L. Lamarque, R. Pal, D. Parker, *Chem. Sci.*, 5, (2014), 1750-1756.
- [6] S.J. Butler, M. Delbianco, L. Lamarque, B.K. McMahon, E.R. Neil, R. Pal, D. Parker, J.W. Walton, J.M. Zwieter, *Dalton Trans.*, 44, (2015), 4791-4803.
- [7] K. Djinic-Carugo, O. Carugo, *J. Inorg. Biochem.*, 143, (2015), 69-76.
- [8] J.M. Zwieter, H. Bazin, L. Lamarque, G. Mathis, *Inorg. Chem.*, 53, (2014), 1854-1866.
- [9] A.D. Sherry, P. Caravan, R.E. Lenkinski, *J. Mag. Res. Im.*, 30, (2009), 1240-1248.
- [10] M. Port, J.-M. Idée, C. Medina, C. Robic, M. Sabatou, C. Corot, *BioMetals*, 21, (2008), 469-490.
- [11] A. Pol, T.R.M. Barends, A. Dietl, A.F. Khadem, J. Eygensteyn, M.S.M. Jetten, H.J.M. Op den Camp, *Env. Microbiol.*, 16, (2014), 255-264.
- [12] J. Keltjens, A. Pol, J. Reimann, H.M. Op den Camp, *Appl. Microbiol. Biotechnol.*, 98, (2014), 6163-6183.
- [13] E. Skovran, N.C. Martinez-Gomez, *Science*, 348, (2015), 862-863.
- [14] E.G. Moore, A.P.S. Samuel, K.N. Raymond, *Acc. Chem. Res.*, 42, (2009), 542-552.
- [15] E.G. Moore, J. Xu, C.J. Jocher, T.M. Corneillie, K.N. Raymond, *Inorg. Chem.*, 49, (2010), 9928-9939.
- [16] L.J. Daumann, D.S. Tatum, B.E.R. Snyder, C. Ni, G.-I. Law, E.I. Solomon, K.N. Raymond, *J. Am. Chem. Soc.*, 137, (2015), 2816-2819.
- [17] R.J. Abergel, A. D'Aléo, C. Ng Pak Leung, D.K. Shuh, K.N. Raymond, *Inorg. Chem.*, 48, (2009), 10868-10870.
- [18] R.J. Abergel, P.W. Durbin, B. Kullgren, S.N. Ebbe, J. Xu, P.Y. Chang, D.I. Bunin, E.A. Blakely, K.A. Bjornstad, C.J. Rosen, D.K. Shuh, K.N. Raymond, *Health Phys.*, 99, (2010), 401-407.
- [19] D.D. An, J.A. Villalobos, J.A. Morales-Rivera, C.J. Rosen, K.A. Bjornstad, S.S. Gauny, T.A. Choi, M. Sturzbecher-Hoehne, R.J. Abergel, *Int. J. Radiat. Biol.*, 90, (2014), 1055-1061.
- [20] B.E. Allred, P.B. Rupert, S.S. Gauny, D.D. An, C.Y. Ralston, M. Sturzbecher-Hoehne, R.K. Strong, R.J. Abergel, *PNAS*, 112, (2015), 10342-10347.
- [21] D.H. Zhu, M.J. Kappel, K.N. Raymond, *Inorg. Chim. Acta*, 147, (1988), 115-121.
- [22] L.C. Uhlir, P.W. Durbin, N. Jeung, K.N. Raymond, *J. Med. Chem.*, 36, (1993), 504-509.
- [23] J. Xu, B. Kullgren, P.W. Durbin, K.N. Raymond, *J. Med. Chem.*, 38, (1995), 2606-2614.
- [24] M. Sturzbecher-Hoehne, B. Kullgren, E.E. Jarvis, D.D. An, R.J. Abergel, *Chem. -Eur. J.*, 20, (2014), 9962-9968.
- [25] J.D. Xu, T.M. Corneillie, E.G. Moore, G.L. Law, N.G. Butlin, K.N. Raymond, *J. Am. Chem. Soc.*, 133, (2011), 19900-19910.
- [26] M.J. Frisch, G.W. Trucks, H.B. Schlegel, G.E. Scuseria, M.A. Robb, J.R. Cheeseman, G. Scalmani, V. Barone, B. Mennucci, G.A.

- Petersson, H. Nakatsuji, M. Caricato, X. Li, H.P. Hratchian, A.F. Izmaylov, J. Bloino, G. Zheng, J.L. Sonnenberg, M. Hada, M. Ehara, K. Toyota, R. Fukuda, J. Hasegawa, M. Ishida, T. Nakajima, Y. Honda, O. Kitao, H. Nakai, T. Vreven, J.A. Montgomery Jr., J.E. Peralta, F. Ogliaro, M.J. Bearpark, J. Heyd, E.N. Brothers, K.N. Kudin, V.N. Staroverov, R. Kobayashi, J. Normand, K. Raghavachari, A.P. Rendell, J.C. Burant, S.S. Iyengar, J. Tomasi, M. Cossi, N. Rega, N.J. Millam, M. Klene, J.E. Knox, J.B. Cross, V. Bakken, C. Adamo, J. Jaramillo, R. Gomperts, R.E. Stratmann, O. Yazyev, A.J. Austin, R. Cammi, C. Pomelli, J.W. Ochterski, R.L. Martin, K. Morokuma, V.G. Zakrzewski, G.A. Voth, P. Salvador, J.J. Dannenberg, S. Dapprich, A.D. Daniels, Ö. Farkas, J.B. Foresman, J.V. Ortiz, J. Cioslowski, D.J. Fox, 2009, Gaussian 09
- [27] M. Dolg, H. Stoll, A. Savin, H. Preuss, *Theor. Chim. Acta*, **75**, (1989), 173-194.
- [28] M. Dolg, H. Stoll, H. Preuss, *Theor. Chim. Acta*, **85**, (1993), 441-450.
- [29] D. Todd, A.E. Martell, 2-Hydroxyisophthalic Acid, John Wiley & Sons, Inc., (2003).
- [30] A.P. Samuel, J. Xu, K.N. Raymond, *Inorg. Chem.*, **48**, (2009), 687-698.
- [31] D.F. Eaton, *Pure Appl. Chem.*, **60**, (1988), 1107-1114.
- [32] C. Würth, D. Geißler, T. Behnke, M. Kaiser, U. Resch-Genger, *Anal. Bioanal. Chem.*, **407**, (2015), 59-78.
- [33] C. Würth, M. Grabolle, J. Pauli, M. Spieles, U. Resch-Genger, *Nat. Protocols*, **8**, (2013), 1535-1550.
- [34] M. Brouwer Albert, *Pure Appl. Chem.*, **83**, (2011), 2213.
- [35] V. Jirsakova, F. Reiss-Husson, I. Agalidis, J. Vrieze, A.J. Hoff, *BBA - Bioenergetics*, **1231**, (1995), 313-322.
- [36] F.L. de Weerd, M.A. Palacios, E.G. Andrizhievskaya, J.P. Dekker, R. van Grondelle, *Biochemistry*, **41**, (2002), 15224-15233.
- [37] E.G. Moore, J. Xu, C.J. Jocher, E.J. Werner, K.N. Raymond, *J. Am. Chem. Soc.*, **128**, (2006), 10648-10649.
- [38] S.I. Weissman, *J. Chem. Phys.*, **10**, (1942), 214-217.
- [39] K. Binnemans, *Chem. Rev. (Washington, DC, U. S.)*, **109**, (2009), 4283-4374.
- [40] J.-C.G. Bünzli, C. Piguet, *Chem. Soc. Rev.*, **34**, (2005), 1048-1077.
- [41] A. D'Aléo, E.G. Moore, G. Szigethy, J. Xu, K.N. Raymond, *Inorg. Chem.*, **48**, (2009), 9316-9324.
- [42] S. Petoud, S.M. Cohen, J.C.G. Bünzli, K.N. Raymond, *J. Am. Chem. Soc.*, **125**, (2003), 13324-13325.
- [43] K. Binnemans, *Coord. Chem. Rev.*, **295**, (2015), 1-45.
- [44] E.G. Moore, J. Xu, C.J. Jocher, I. Castro-Rodriguez, K.N. Raymond, *Inorg. Chem.*, **47**, (2008), 3105-3118.
- [45] A.P.S. Samuel, J. Xu, K.N. Raymond, *Inorg. Chem.*, **48**, (2008), 687-698.
- [46] R.M. Supkowski, W.D. Horrocks, *Inorg. Chim. Acta*, **340**, (2002), 44-48.
- [47] A. Beeby, I. M. Clarkson, R. S. Dickens, S. Faulkner, D. Parker, L. Royle, A. S. de Sousa, J. A. Gareth Williams, M. Woods, *J. Chem. Soc., Perkin Trans. 2*, (1999), 493-504.
- [48] A. D'Aléo, E.G. Moore, J. Xu, L.J. Daumann, K.N. Raymond, *Inorg. Chem.*, **54**, (2015), 6807-6820.
- [49] M.H.V. Werts, R.T.F. Jukes, J.W. Verhoeven, *Phys. Chem. Chem. Phys.*, **4**, (2002), 1542-1548.
- [50] A. Beeby, L.M. Bushby, D. Maffeo, J.A. Gareth Williams, *J. Chem. Soc., Dalton Trans.*, (2002), 48-54.
- [51] M.P. Hehlen, M.G. Brik, K.W. Krämer, *J. Lumin.*, **136**, (2013), 221-239.
- [52] B.R. Judd, *Physical Review*, **127**, (1962), 750-761.
- [53] G.S. Ofelt, *J. Chem. Phys.*, **37**, (1962), 511-520.
- [54] C. Doffek, M. Seitz, *Angew. Chem. Int. Ed.*, **54**, (2015), 9719-9721.
- [55] S.K. Ghorai, S.K. Samanta, M. Mukherjee, S. Ghosh, *The J. Phys. Chem. A*, **116**, (2012), 8303-8312.
- [56] S.K. Ghorai, S.K. Samanta, M. Mukherjee, P. Saha Sardar, S. Ghosh, *Inorg. Chem.*, **52**, (2013), 1476-1487.
- [57] S.K. Samanta, S.M.T. Abtab, P.S. Sardar, S. Sanyal, M. Chaudhury, S. Ghosh, *Eur. J. Inorg. Chem.*, **2014**, (2014), 3101-3113.
- [58] T.J. Sorensen, A.M. Kenwright, S. Faulkner, *Chem. Sci.*, **6**, (2015), 2054-2059.

Highlights

- 2-Hydroxyisophthalamide (IAM) and 1,2-hydroxypyridonate (HOPO) mixed ligands are prepared
- Photophysical properties of Tb and Eu complexes are reported
- When bound to a primary amine the above chromophores are better in sensitizing Tb and Eu